Chapter 6

Atmospheric Pressure Chemical Vapor Deposition of Graphene

Phuong V. Pham

Additional information is available at the end of the chapter

http://dx.doi.org/10.5772/intechopen.81293

Abstract

Recently, graphene has gained significant interest owing to its outstanding conductivity, mechanical strength, thermal stability, etc. Among various graphene synthesis methods, atmospheric pressure chemical vapor deposition (APCVD) is one of the best syntheses due to very low diffusivity coefficient and a critical step for graphene-based device fabrication. High-temperature APCVD processes for thin film productions are being recognized in many diversity technologies such as solid state electronic devices, in particular, high quality epitaxial semiconductor films for silicon bipolar and metal oxide semiconductor (MOS) transistors. Graphene-based devices exhibit high potential for applications in flexible electronics, optoelectronics, and energy harvesting. In this chapter, recent advances of APCVD-based graphene synthesis and their related applications will be addressed.

Keywords: graphene, atmospheric pressure chemical vapor deposition (APCVD), single-layer graphene (SLG), bilayer graphene (BLG), atmosphere pressure, large-scale

1. Introduction

Single-layer graphene (SLG), bilayer graphene (BLG), and multi-layer graphene (MLG) films have been regarded as optimal materials for electronics and optoelectronics owing to their excellent electrical properties and their ability to integrate with current top-down device fabrication technology [1–95]. Since the beginning of the twenty-first century, the interest in graphene materials has drastically increased, which is apparent in the number of annual publications on graphene (**Figure 1**). Until now, various strategies including chemical vapor deposition (CVD) [28], liquid and mechanical exfoliation from graphite [23, 29, 30], epitaxial growth on crystal substrate [31–34], or solution-based processes on graphene oxides (GOs)

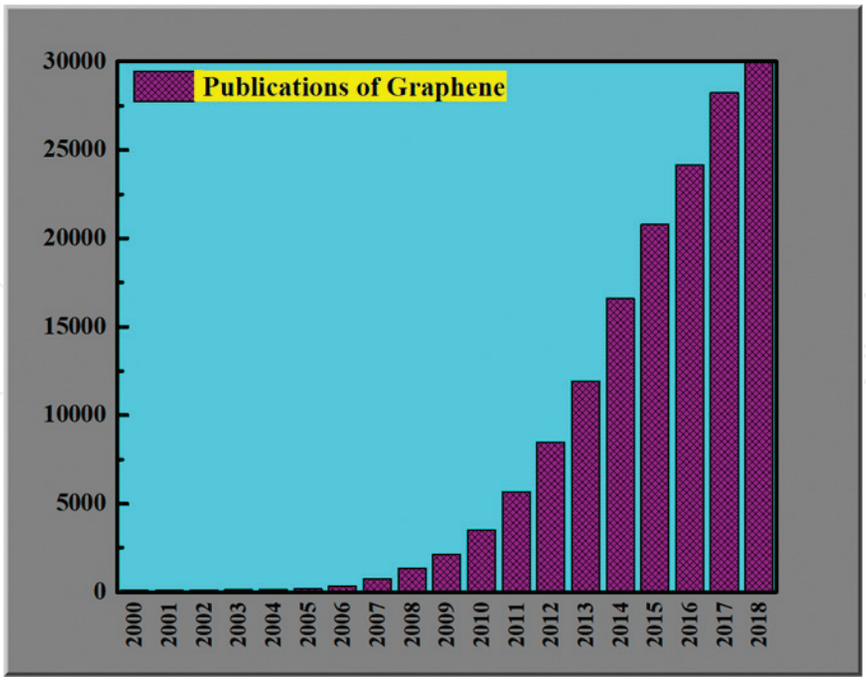

Figure 1. Graphene publications from 2000 to 2018. Source: ISI Web of Science (search: Topic = Graphene).

[35–41]. They have been investigated for obtaining graphene layers. In particular, recent advances in CVD growth have successfully led to large-scale graphene production on metal substrates [1, 27, 42–48], driven by the high demand for utilizing graphene in possible applications of current complementary metal-oxide-semiconductor (CMOS) technology such as radio-frequency transistors, optical devices, and deposition processes [2].

High-quality large-scale graphene has been synthesized on conducting metallic substrates by using the catalytic CVD growth approach, which promoted a wide range of graphene-based device applications [1, 28, 42–49]. However, graphene grown on a metal substrate needs to be transferred onto dielectric substrates for electronic applications. Although various approaches, such as wet etching/transfer [45], mechanical exfoliation/transfer [23, 29, 30], bubbling transfer [50], electrochemical delamination [51–53], for transferring from the catalytic metal growth substrates to dielectric device substrates have been developed; none of these approaches is free from degradation of the transferred graphene. For example, 'wet etching and transfer,' the most widely used transfer approach, is a serial process, which includes encapsulation of the graphene surface with polymer support.

Growing through CVD is for the production of films or for coating of metal, semiconductor, crystalline, and vitreous formed-compounds in either, occupying high-purity as well as desirable characteristics. In addition, the creation of controllable film with varying stoichiometry results CVD uniquely among deposition approaches. Other advantages include reasonably low cost of the equipment and operating expenses, suitability for semicontinuous operation. Consequently, the variants of CVD have been developed recently such as low-pressure chemical vapor deposition (LPCVD), APCVD, plasma-enhanced chemical vapor deposition (PECVD), and laser-enhanced chemical vapor deposition (LECVD). The hybrid system represents for both CVD and physical vapor deposition (PVD) have also discovered.

Among the utilized synthesis methods, APCVD has been considered as the most potential and medium cost one for large-scale high-quality graphene on various metallic substrates including Pt [54], Ir [42], Ni [7], and Cu [45]. Especially, Cu is considered as the best choice owing to low-carbon solubility, well-controlled surface, and inexpensive for growing monolayer graphene [45, 55]. Many efforts have made for obtaining large-scale single crystal graphene with as less grain boundaries as possible. There are two general methods to realize: the first method associates with the growth of single domains with possible enlargement [54, 56–63]. Despite the centimeter-scale domains have achieved, this method is not the bright candidate in practice for large-scale growth because of the difficult quantity control of nucleation seeds as well as unclear self-limiting growth factors resulting worse and requiring very long growth time (over 24 h) [64, 65]. The second method is the alignment of graphene domain orientations on arbitrary substrates and then to atomically stitch them to form uniform single crystalline graphene [5, 66]. This seems to be ideal for growing large scale.

The CVD method creates large-scale graphene but polycrystalline morphology, which includes different oriented domains. Such the orientated disorders inevitably lead to graphene grain boundaries (GGBs) formation at intercalated interface of domain [67–69]. GGBs include a series of nonhexagonal rings of pentagons, heptagons, and octagons. Intrinsic graphene has high conductivity and chemical inert, however, the appearance of atomically defect lines and GGBs in graphene could remarkably modulate its features such as mechanics [69, 70], electrics [71, 72], chemistry [73, 74], and magnets [75]. These defect lines have extraordinary features and rely on the atomical configuration at GGBs and the crystallinity of mono-grains; moreover, they could be modulated through different function groups [75]. Therefore, the investigation on the orientations and boundaries of the grains is the key to comprehend the underlying features as well as to realize compatible applications of graphene.

Conventionally, graphene is grown on metal foils (Cu, Ni, Pt, etc.) through APCVD, LPCVD, or PECVD. The temperatures, pressures, and concentrations of precursor gases inside the furnace play key roles on the graphene growth and quality. These factors need be optimized to get the desirable growth results. In general, surface morphology is studied via optical microscope (OM) and scanning electron microscopy (SEM); the graphene quality is examined through Raman spectra, UV-visible spectroscopy, and transmission electron microscopy (TEM); and sheet resistance (R_s) of synthesized graphene is measured utilizing four-point probe technique. Almost graphene films synthesized via APCVD are monolayer with better quality in atmospheric condition compared with LPCVD or PECVD. The synthesis study using APCVD would be greatly significant in the desirable growth of graphene and other related materials. In this chapter, recent advances of APCVD-based graphene synthesis with practical concerns about chemical vapor transport, deposition process as well as their device applications will be addressed.

2. Growth mechanism of APCVD-based graphene

APCVD growth of graphene is a chemical synthesis process at atmosphere pressure for the formation of SLG or FLG on an arbitrary substrate by exposing the substrate to the gas-phase

precursors at controlled reaction conditions [76]. Owing to the versatile nature of APCVD, intricately mixed homogeneous gas-phase and heterogeneous surface reactions are involved [77]. In general, as the partial pressure and/or temperature in the reaction substances are increased, homogeneous gas-phase reactions and the resulting homogeneous nucleation became significant [77]. To grow a high-quality graphene layer, this homogeneous nucleation needs to be minimized [77]. A general mechanism for APCVD-based graphene growth on catalytic metal substrates, for the growth of uniform and highly crystalline graphene layer on the surface, includes eight steps as follow: (1) mass transport of the reactant, (2) reaction of the film precursor, (3) diffusion of gas molecules, (4) adsorption of the precursor, (5) diffusion of the precursor into substrate, (6) surface reaction, (7) desorption of the product, and (8) removal of the by-product (**Figure 2**) [78, 96].

It has been a general observation in most of the experimental works that the LPCVD produces nonuniform thick graphene layers. However, as high-quality single-layer graphene growth, APCVD would be a better choice due to reduced mean free path/diffusion coefficient of the reactive species on the catalyst [79]. APCVD shows a much lower diffusivity coefficient: $D_g \sim 1/(\text{total pressure})$ compare with LPCVD. As the result, the small multilayer graphene islands is less appearing on a full large monolayer graphene island via APCVD growth process [79] compared with LPCVD.

In another graphene growth mechanism model, hydrocarbon molecules are absorbed as well as dissociated on Cu forming active carbon species by dehydrogenation reaction (**Figure 3**). These species are diffused on two sides of Cu foil and agglomerated on its active sites to form graphene nucleation seeds. Actually, introducing H_2 gas is mandatory as a key role in graphene growth for most CVD approaches. The overall processes of graphene growth on Cu are described (**Figure 3**) [89]. Generally, there are three main expected steps: (i) adsorp-decompose, (ii) diffuse-desorb, and (iii) nucleate-grow (**Figure 3**) [89]. The active carbon species are commonly not stable and easily agglomerate with thermodynamically stable species on active sites to form graphene nucleation seeds by the reactions: $(CH_x)_s$ + graphene ➔ (graphene-C) + $(CH_x)_s$ with x = 1, 2, 3 [89]. Till those

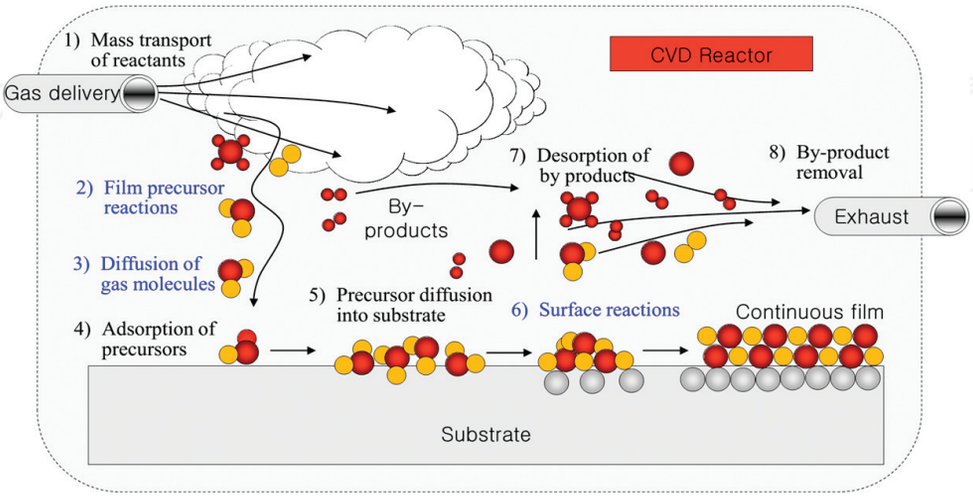

Figure 2. Diagram of CVD growth mechanism (APCVD and LPCVD) of graphene: transport and reaction processes. Reproduced with permission from [78, 96]. Copyright 2011, Freund Publishing.

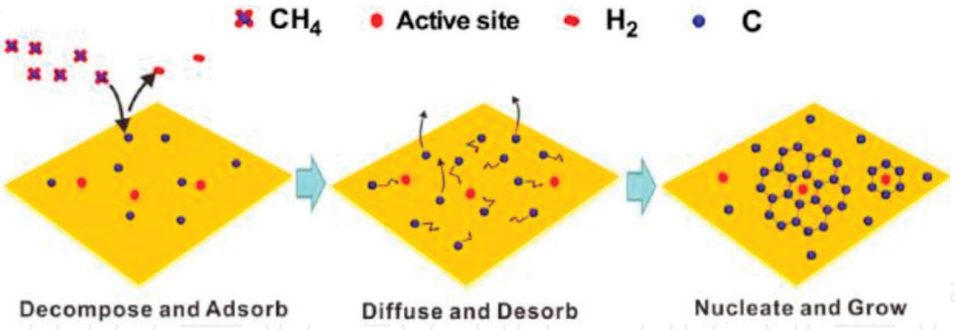

Figure 3. Schematic for graphene growth mechanism on Cu substrate. Reproduced with permission from [89]. Copyright 2012, American Chemical Society.

seeds formed, almost the active carbon species are incorporated and captured at surface/interface of graphene lattice. In addition, H_2 precursor plays more role as an etchant and controls the size as well as shape of graphene domains via reactions: H_s + graphene ➔ (graphene-C) + $(CH_x)_s$ with x = 1, 2, 3 [89].

Typically, APCVD growth of 2D materials (e.g. graphene) involves catalytic activation of chemical reactions of precursors at the growth substrate surface/interface in a properly designed environment. In general, the roles of precursors, conditions (e.g. fast growth rates, large domain size, or very high crystalline quality), atmosphere, substrates, and catalysts are the key factors affecting the final quality of the grown 2D materials. So far, significant efforts have been made to prepare high crystalline 2D materials (e.g. graphene), but many challenges are still ahead. For example, due to the rough feature of catalytic metal surface, growth of uniform and high-quality graphene is considerably difficult. The 2D material research community is also interested in new precursors (e.g. solid precursor only, gas precursor, or solid precursor mixed with certain solvents) that could form uniformly high-quality graphene with minimal defect density. Another question is the effect of growth rate on the catalytic metal surface on the quality of graphene. Currently, it is difficult to give an exact answer, as investigations are progressing at an exponential rate. To date, the understanding of the concept of the general mechanism of the APCVD growth of graphene is still not yet adequate, neither experimentally nor theoretically. Thus, understanding the graphene growth mechanism and the effect of various growth conditions will be of significant interest to the 2D material research community to obtain large scale, high-quality graphene.

3. APCVD growth of graphene

CVD is a thin solid film deposition process of vapor species through suitable chemical reaction. The deposition needs low-carbon solubility substrate in high-temperature region [80]. To date, CVD is the sole approach, which could produce high-quality graphene with ultra-large size [45, 81]. For the first experiment, researchers successfully synthesized graphene films via CVD on Ni and Cu catalytic substrates [44, 82, 83]. The significant progress for large-size and high-quality graphene films has also well done [81, 83].

APCVD requires high temperature (~1000°C) for graphene synthesis. It is experimentally expensive; therefore, it requires the CVD equipment more sophisticatedly. Unfortunately, this is an obstacle for direct-growth of graphene on insulating device substrate (e.g., SiO_2), for instance, it can produce unavoidable physical damages around 1000°C and dramatically degrades the quality of synthesized graphene. As a result, the deposition of graphene on insulating substrates at reduced temperatures becomes very necessary [84, 85]. The features of graphene will change corresponding with the number of layers. Hence, the electronic, optical, mechanical, and other features of graphene could be tuned by controlling the number of layers, or by adjusting the experimental conditions. Currently, it is still the challenge to exactly atomic-scale control the number of graphene layers [86–88]. The proposed synthesis method is composed by four stages (cleaning, precursor injection, reaction time, and cooling). The temperature and flow rate of carbon precursor were the studied parameters. In **Figure 4a**, **b**, the common CVD systems and differences are shown [90].

In 2016, Wang et al. obviously showed millimeter-scale graphene single crystals synthesized on Cu through APCVD (**Figure 5**) [91]. The possible mechanism will be based on graphene nucleation and kinetic growth. At the stage of nucleation, thermal decomposition of oxide layer leads to O_2 desorption at high temperature at front side of Cu and dominates the temperature dependence of nucleation density. The graphene island growth is edge-limited on two sides of Cu at various enlargement rates. The roughness of support substrates (quartz, sapphire) also affects the graphene deposition. After optimized annealing and polished

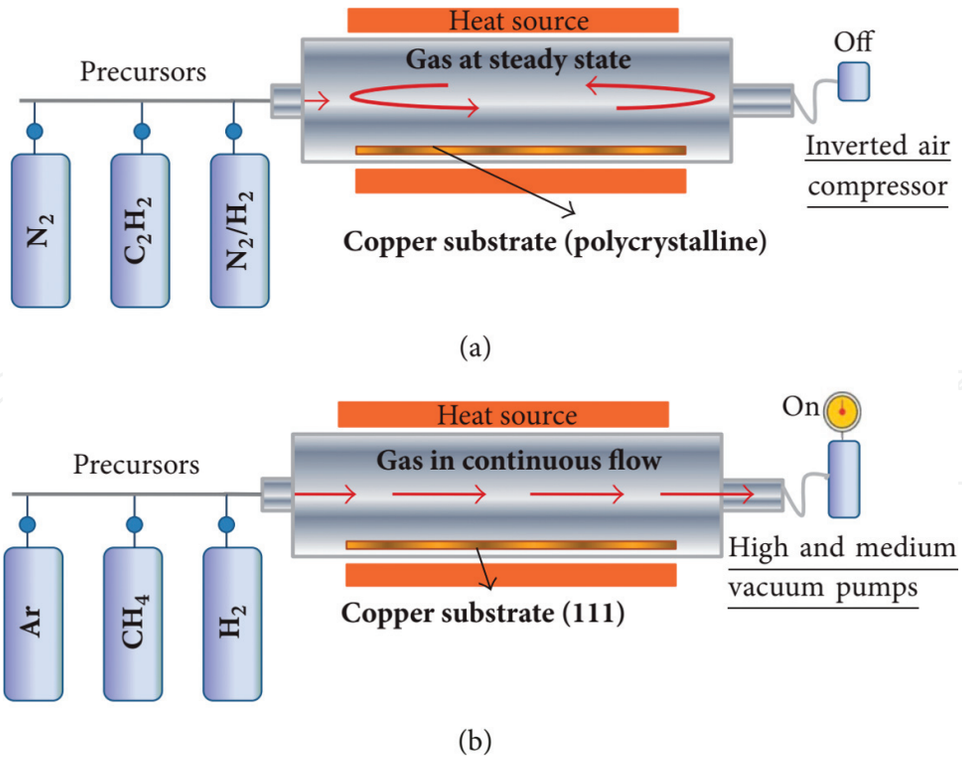

Figure 4. Schematic of graphene synthesis by (a) APCVD using polycrystalline Cu substrate and gas discontinuous flow and (b) high vacuum using single crystalline Cu(111) substrate and gas continuous flow. Reproduced with permission from [90]. Copyright 2018, Hindawi Publishing.

http://dx.doi.org/10.5772/intechopen.81293

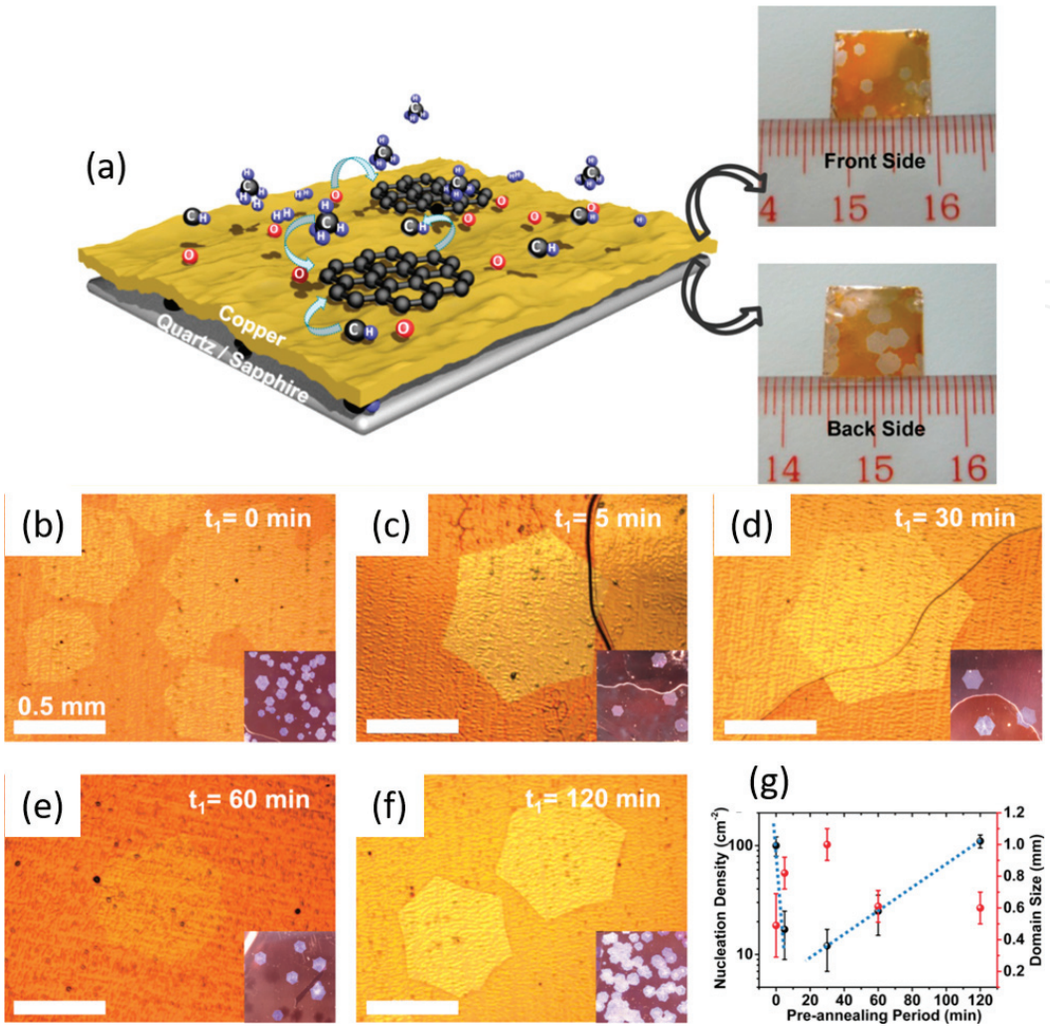

Figure 5. (a) Schematic for APCVD-grown graphene on Cu located on quartz or sapphire substrates. Insets in (a) are OM images of graphene/Cu at front side and back side. OM images of grown graphene on Cu foils with various pre-annealing times of (b) 0, (c) 5, (d) 30, (e) 60, (f) 120 min at the same growth time (60 min). (g) Evolution of nucleation density and size of graphene domains as a function of pre-annealing times. Reproduced with permission from [91]. Copyright 2016, American Chemical Society.

support substrate, the isolated graphene islands (~3 mm) were produced with a growth rate (25 μm/min). The domains were uniformly single-crystalline graphene with good mobility (~4900 cm^2/V.s) at room temperature. **Figure 5b-f** shows OM images of graphene domains/Cu for 60 min growth at various Ar pre-annealing times. The growth and cooling parameters maintained the same. Here, the Ar heating induced the growth of individual graphene domains with relatively low nucleation density (102 cm^{-2}) owing to the catalyst passivation of oxide layer on top of Cu. Through annealing in 30 min (**Figure 5d**), the nucleation density reduced ~12 nuclei/cm^2, and a grain size of ~1 mm was obtained after 60 min growth (**Figure 5e**). But the extending of annealing (120 min) caused the increase of nucleation density with reduced domain size (~0.6 mm) (**Figure 5f**). The evolutions of nucleation densities and domain sizes via annealing are shown in **Figure 5g**. The nucleation density reveals a nonmonotonic dependence of Ar-passivated annealing. Since the surface becomes flatter after

annealing, the O-species also gradually desorb at surface, which leaves pristine Cu as active nucleation sites following the growth steps.

Thermodynamics of CVD-based graphene synthesis using catalytic Cu at particular temperature is same irrespective at atmosphere pressure (AP), low pressure (LP), or ultrahigh vacuum (UHV) [79]. But, the kinetics will vary on different steps. The kinetics of cooling rate, the pressure of CVD furnace has major ramification on the graphene growth rate, large-scale thickness uniformity, and the defect density. **Figure 6A** illustrates a steady state flow of a mixture of CH_4, H_2, and Ar precursors on Cu surface at ~1000°C [79]. The boundary layer because of steady state gas flow is stagnant. Firstly, the carbon species (1) diffuse via the boundary layer to the surface, then (2) will be adsorbed on the surface, (3) decompose for formation of active carbon species, (4) diffuse on/into the catalyst surface and forming the graphene lattice, (5) inactive species (e.g. H_2) get desorbed, forming H_2, then (6) diffuse away through boundary layer and swept away by the bulk gas flow [79]. Processes, which occur on/close the surface, are highly affected by substrate temperature. Generally, there are two fluxes of active species: flux of active species via boundary layer and at metal substrate surface forming graphene lattice (**Figure 6B**) [79]. The equations of these fluxes are $F_{mass\ transport} = h_g(C_g - C_s)$ and $F_{surface\ reaction} = K_sC_s$ where, $F_{mass\text{-}transport}$ is the flux of active species through the boundary layer, $F_{surface\text{-}reaction}$ is the flux of consumed active species at surface, h_g is the mass transport coefficient, K_s is the surface reaction constant, C_g is the concentration of gas in bulk, and C_s is the concentration of active species at the surface [79]. At high temperatures, under APCVD parameters, mass transport via boundary layer is rate limiting ($K_s \gg h_g$), and under LP and UHV parameters, the surface reaction is the rate limiting step ($h_g \gg K_s$) [79].

A diagram of designed-APCVD for graphene synthesis is described in **Figure 7**. This splits one gas inlet in two paths by means of glass valves: one for heating, annealing, and cooling (P1); and the other for graphene synthesis (P2). The synthesis temperature is 980–990°C in tubular furnace; during heating, the Ar-H_2 (5% of H_2) flow is 0.2 l/min via P1. Then Cu is annealed in 20–30 min. Then, the flow passed via alcohol container (P2) to desired growth rate, and the varied time depended on precursor type. Keeping the flow rate, the flux is to P1 and the sample is annealed in 10 min. As the result, this annealing step improved the graphene quality

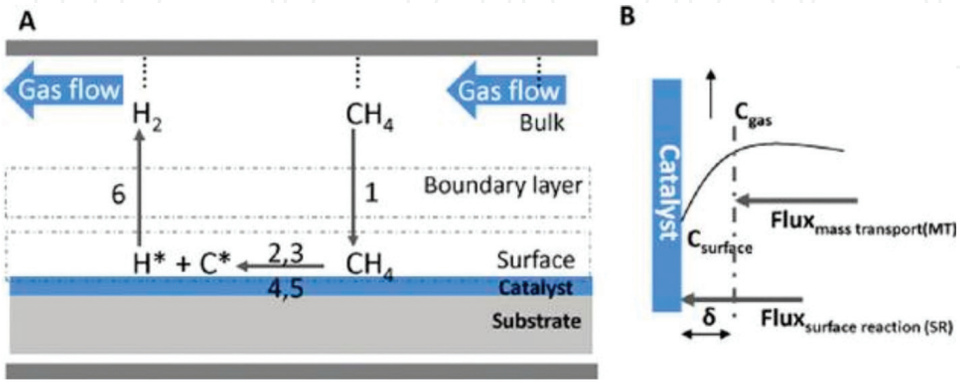

Figure 6. (A) Schematic for graphene growth mechanism using low carbon solid solubility catalysts (Cu) at atmosphere pressure (AP), low pressure (LP), or ultrahigh vacuum (UHV) environments. (B) Mass transport and surface reaction fluxes under steady state conditions. Reproduced with permission from [79]. Copyright 2010, American Chemical Society.

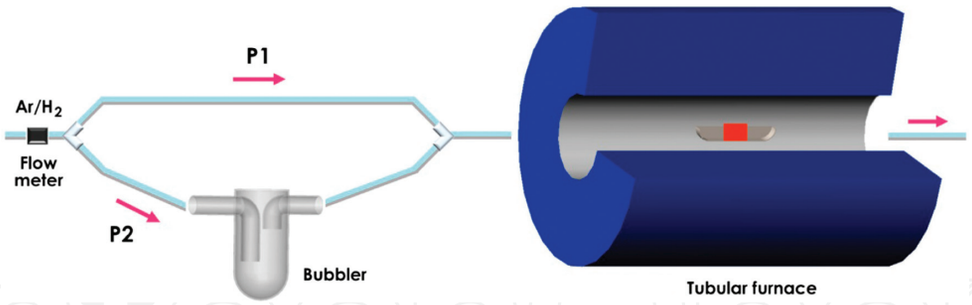

Figure 7. Graphene growth mechanism on new designed APCVD with a bubbler. A single gas inlet is split into two paths (P1 and P2) using glass. During heating/annealing/cooling, gas is passed through P1; while for graphene growth, gas flows through P2 and bubbler containing alcohol. Inside the tubular furnace a combustion boat is placed in the center containing a Cu foil. Reproduced with permission from [92]. Copyright 2013, Elsevier.

a lot. The temperature, the time, and flow rate permit a sophisticated controlling on carbon concentration toward tubular furnace (**Figure 7**) [92].

The additional oxide substrate (SiO_2, Al_2O_3) to continuously supply the oxygen (O_2) to Cu surface of APCVD graphene synthesis (**Figure 8a,b**) [93]. Cu was placed on oxide substrates away in 15 μm gap. Last report proved that the oxide shall slowly release O_2 at above 800°C) [97]. To clear it, Xu et al. carried out Auger electron spectroscopy (AES) element measurement on SiO_2, as the result, O_2 escaped from SiO_2 after annealing in UHV or CVD (**Figure 8c**) [93]. Despite the small amount of O_2 released, the O_2 concentration between the narrow gap (15 μm) of Cu and oxide substrate could be high because of the trapping effect; hence, the O_2 attachment to Cu surface significantly trapped. Beside AP condition, high CH_4 flow (5 sccm) and high CH_4/H_2 ratio (∼1) ensure a sufficient supply of carbon for ultrafast domain synthesis. The large domains (∼0.3 mm) appeared on the back surface of Cu (**Figure 8d**). Contrarily, graphene domains at front surface of Cu are 20 times smaller (∼15 μm) (**Figure 8e**). All these domains are star-shaped. For further demonstration, when graphite is used as the supporting substrate, graphene domains on both sides of Cu are also star-shaped similar with the case of SiO_2 (**Figure 8g**) [93].

Figure 8h,i revealed OM images of graphene/Cu in 60 and 80 min under CH_4 0.000075 Pa [94]. The graphenes needed to place in air (200°C, 1 min) for chemical oxidation between Cu and air to emerge the nonoxidized-graphene domains for the observation by OM and human-eye. Graphene partly covered the Cu (∼70%) after 60 min. Some isolated domains were ∼1.5 mm (**Figure 8h**) [94]. But the color as well as contrast of sample were of no change after 80 min implying that Cu got full coverage by graphene via OM image (**Figure 8i**) [94]. The histogram in **Figure 8j** showed the growth distribution of domain sizes for 50–60 min [94]. The distribution of domain sizes increased via growth time; the domain sizes were 0.4–0.8 mm for 50–60 min. The time evolution of average domain size and coverage were clearly described in **Figure 8k** [94]. The domain sizes for 100% coverage after 80 min was ∼1 mm [94].

A growth at APCVD in Mohsin et al. is to avoid Cu evaporation from the foil substrate, which commonly appears in LPCVD case [95, 98]. Regarding **Figure 9,** firstly Cu is placed on a tungsten (W) foil for preventing the dewetting of liquid Cu on quartz. Then, it was heated up 1100°C, which is higher melting point of Cu for 30 min under Ar (940 sccm) and H_2 (60 sccm).

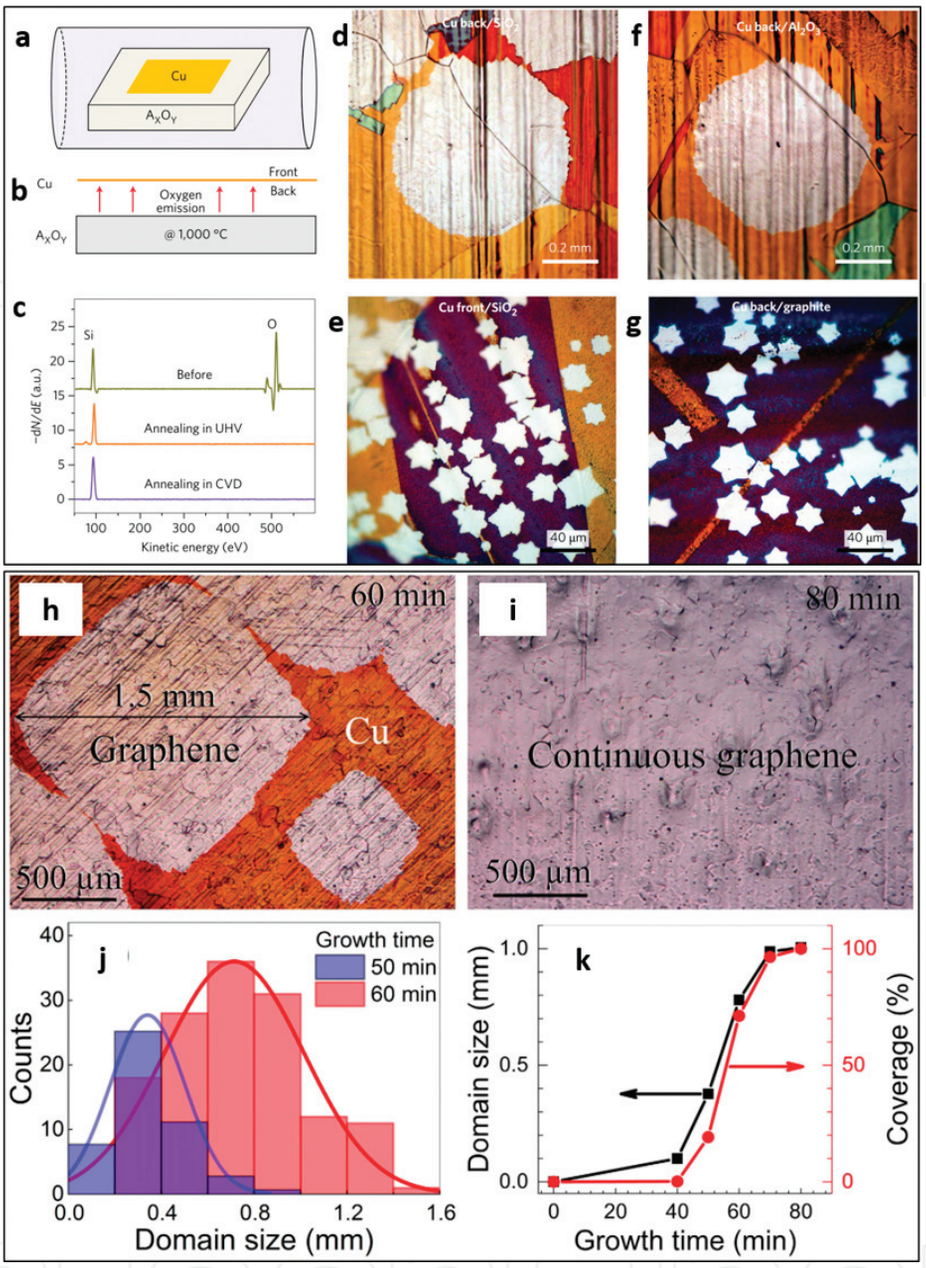

Figure 8. (a) Schematic of graphene growth on Cu using O_2-assisted APCVD. (b) Side view of (a). (c) Auger electron spectroscopy (AES) of SiO_2 before/after annealing at 1000°C in UHV and APCVD systems. The disappearance of O_2 peak after annealing proves the emission of O_2 from the oxide at high temperature. (d, e) OM images of graphene domains on the back (d) and front (e) Cu surfaces using fused silica as the supporting substrate. (f, g) OM images of graphene domains on the back Cu surfaces using sapphire (Al_2O_3) (f) or graphite (g). Reproduced with permission from [93]. Copyright 2016, Nature Publishing Group. (h, i) OM images of graphene/Cu after 60 and 80 min, respectively. APCVD conditions: 1 atm, 1030°C, 0.3 sccm CH_4, 80 sccm H_2, and 3920 sccm Ar. (j) Histogram of domain size for 50 and 60 min growth. (k) The graphene coverage and the average domain size as a function of growth time. Reproduced with permission from [94]. Copyright 2016, Nature Publishing Group.

Then, the temperature is lowered to 1075°C, and the Cu resolidified. Growth was carried out at this temperature, with 0.1% dilute CH_4 in Ar. On the right side of **Figure 9**, it shows OM image of two hexagon domains of graphene (>1 mm) which has similar morphology [95]. These domains obtained in Mohsin et al. are hexagons with very less roughness edges compared to previous reports [60, 89].

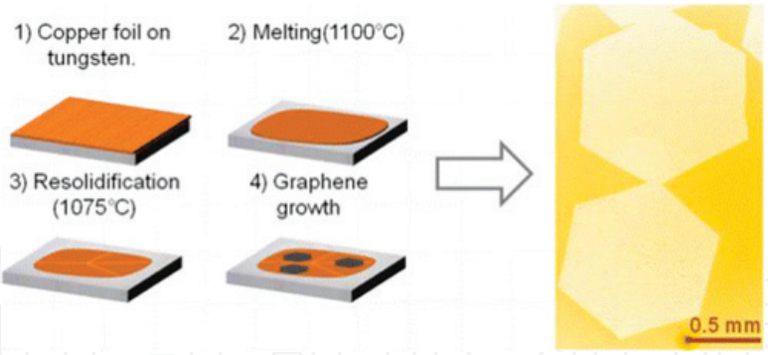

Figure 9. (a) Simple method to grow millimeter-size graphene single crystals on melted and resolidified Cu using APCVD. (b) OM image of the synthesized graphene domains. Reproduced with permission from [95]. Copyright 2013, American Chemical Society.

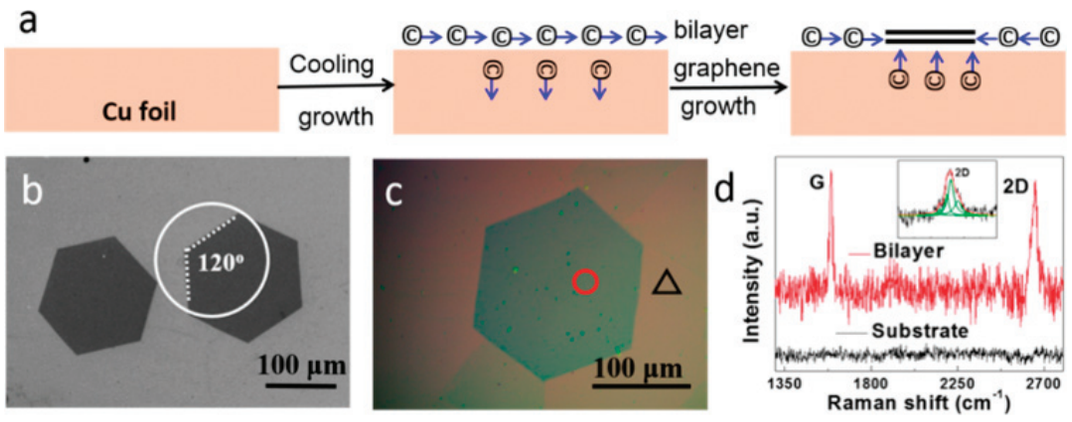

Figure 10. (a) Schematic of bilayer graphene growth using a cooling APCVD. (b, c) SEM and OM images of bilayer graphene domains, respectively. (d) Rama spectra of bilayer graphene. Reproduced with permission from [99]. Copyright 2016, American Chemical Society.

APCVD-based bilayer graphene growth is another great issue for optimum electronic and photonic devices because of higher carrier mobility and wider band gap by perpendicular electric field compared with single-layer graphene [99, 100]. The synthesis of bilayer graphene faced many drawbacks owing to limited grain size and nonsynchronic growth between the first and the second graphene layer. In 2016, Sun et al. reported a cooling-APCVD to growth of bilayer graphene on polycrystalline Cu (**Figure 10**) [99]. Here, the surface adsorption for decomposed carbons and phase segregation for dissolved carbon were shown. Consequently, the millimeter-scale hexagonal bilayer graphene (~1.0 mm) was produced. This study opens the possibility to grow centimeter-scale bilayer graphene for optimum graphene-based applications in recent future.

4. Conclusions

Strategies for direct graphene growth using APCVD method have been reviewed. The prospects of APCVD-grown graphene are bright and currently receiving considerable attention

from the 2D material research community. Yet, understanding the growth process and conditions that affect the quality of graphene is not adequate.

Because APCVD growth depends on thermal decomposition of carbon resource, the growth rate is usually low and size of the graphene domain is small, resulting in growth of defective graphene layer. To date, the challenge remains for this research directions and large-scale high-quality graphene productions are still hard. In order to obtain more advanced results, an in-depth mechanism understanding of APCVD-based graphene growth is essential.

Cu is considered as the best substrate owing to low-carbon solubility, well-controlled surface, and inexpensive for growing monolayer graphene. Generally, graphene is synthesized on Cu via APCVD parameters utilizing CH_4 precursor revealed that the growth is different from single layer graphene at low CH_4 concentration to multi-layer domain on a single layer at higher CH_4 concentration. In particular, APCVD-based graphene growth at higher CH_4 concentration has no self-limiting compared with LPCVD, indicating that further investigation is needed to point out the growth mechanism. The kinetic processes utilizing low carbon solubility catalyst via APCVD parameters were presented.

Finally, APCVD-grown graphene on flexible/metal/dielectric substrates assisted by metal powder precursors (solid, gas, and solution) contained inside a sub-chamber for direct evaporation into an innovative APCVD main chamber allowing hexagonal domain formation on flexible/metal/dielectric substrates is the secret topic and needs to be exploited in the coming time.

Conflict of interest

There are no conflicts of interest to declare.

Author details

Phuong V. Pham[1,2]*

*Address all correspondence to: pvphuong@skku.edu

1 SKKU Advanced Institute of Nano Technology (SAINT), Sungkyunkwan University (SKKU), Suwon, Gyeonggi-do, South Korea

2 Center for Multidimensional Carbon Materials, Institute for Basic Science, Ulsan, South Korea

References

[1] Kim KS, Zhao Y, Jang H, Lee SY, Kim JM, Kim KS, et al. Large-scale pattern growth of graphene films for stretchable. Nature. 2009;**457**:706-710. DOI: 10.1038/nature07719

[2] Kim K, Choi JY, Kim T, Cho SH, Chung HJ. A role for graphene in silicon-based semiconductor devices. Nature. 2011;**479**:338-344. DOI: 10.1038/nature10680

[3] Duong DL, Han GH, Lee SM, Gunes F, Kim ES, Kim ST, et al. Probing graphene grain boundaries with optical miscroscopy. Nature. 2012;**490**:235-239. DOI: 10.1038/nature11562

[4] Choi J-Y. Graphene transfer: A stamp for all substrates. Nature Nanotechnology. 2013;**8**: 311-312. DOI: 10.1038/nnano.2013.74

[5] Lee JH, Lee EK, Joo WJ, Jang Y, Kim BS, Lim JY, et al. Wafer-scale growth of single-crystal monolayer graphene on reusable hydrogen-terminated germanium. Science. 2014;**344**: 286-289. DOI: 10.1126/science.1252268

[6] Shin HJ, Choi WM, Yoon SM, Han GH, Woo YS, Kim ES, et al. Transfer-free growth of few-layer graphene by self-assembled monolayers. Advanced Materials. 2011;**23**:4392-4397. DOI: 10.1002/adma.201102526

[7] Chae SJ, Güneş F, Kim KK, Kim ES, Han GH, Kim SM, et al. Synthesis of large-area graphene layers on poly-nickel substrate by chemical vapor deposition: Wrinkle formation. Advanced Materials. 2009;**21**:2328-2333. DOI: 10.1002/adma.200803016

[8] Güneş F, Shin HJ, Biswas C, Han GH, Kim ES, Chae SJ, et al. Layer-by-layer doping of few-layer graphene film. ACS Nano. 2010;**4**:4595-4600. DOI: 10.1021/nn1008808

[9] Pham VP, Jang HS, Whang D, Choi JY. Direct growth of graphene on rigid and flexible substrates: Progress, applications, and challenges. Chemical Society Reviews. 2017;**46**: 6276-6300. DOI: 10.1039/c7cs00224f

[10] Pham VP. A library of doped-graphene images via transmission electron microscopy. C. 2018;**4**:34. DOI: 10.3390/c4020034

[11] Pham VP, Nguyen MT, Park JW, Kwak SS, Nguyen DHT, Mun MK, et al. Chlorine-trapped CVD bilayer graphene for resistive pressure sensor with high detection limit and high sensitivity. 2D Materials. 2017;**4**:025049. DOI: 10.1088/2053-1583/aa6390

[12] Pham VP, Kim KN, Jeon MH, Kim KS, Yeom GY. Cyclic chlorine trap-doping for transparent, conductive, thermally stable and damage-free graphene. Nanoscale. 2014;**6**: 15301-15308. DOI: 10.1039/c4nr04387a

[13] Pham VP, Kim KH, Jeon MH, Lee SH, Kim KN, Yeom GY. Low damage pre-doping on CVD graphene/Cu using a chlorine inductively coupled plasma. Carbon. 2015;**95**: 664-671. DOI: 10.1016/j.carbon.2015.08.070

[14] Pham VP, Mishra A, Yeom GY. The enhancement of hall mobility and conductivity of CVD graphene through radical doping and vacuum annealing. RSC Advances. 2017;**7**: 16104-16108. DOI: 10.1039/c7ra01330b

[15] Pham VP. Cleaning of graphene surfaces by low pressure air plasma. Royal Society Open Science. 2018;**5**:172395. DOI: 10.1098/rsos.172395

[16] Pham VP, Kim DS, Kim KS, Park JW, Yang KC, Lee SH, et al. Low energy BCl3 plasma doping of few-layer graphene. Science of Advanced Materials. 2016;**8**:884-890. DOI: 10.1166/sam.2016.2549

[17] Kim KN, Pham VP, Yeom GY. Chlorine radical doping of a few layer graphene with low damage. ECS Journal of Solid State Science and Technology. 2015;**4**:N5095-N5097. DOI: 10.1149/2.0141506jss

[18] Pham VP. Chemical vapor deposited graphene synthesis with same-oriented hexagonal domains. Engineering Press. 2018;**1**:39-42. DOI: 10.28964/EngPress-1-107

[19] Pham VP. How can the nanomaterial surfaces be highly cleaned? Edelweiss Applied Science and Technology. 2018;**2**:184-186

[20] Pham VP. Layer-by-layer thinning of 2D materials. Edelweiss Applied Science and Technology. 2018;**2**:36-37

[21] Pham VP. Plasma-related graphene etching: A mini review. Journal of Materials Science and Engineering with Advanced Technology. 2018;**17**:91-106. DOI: 10.18642/jmseat_7100121943

[22] Pham VP. Graphene Etching: How Could it be Etched? Current Graphene Science; 2018 (Accepted)

[23] Geim AK, Novoselov KS. The rise of graphene. Nature Materials. 2007;**6**:183-191. DOI: 10.1038/nmat1849

[24] Neto AHC, Guinea F, Peres NMR, Novoselov KS, Geim AK. The electronic properties of graphene. Reviews of Modern Physics. 2009;**81**:109-162. DOI: 10.1103/RevModPhys.81.109

[25] Schwierz F. Graphene transistor. Nature Nanotechnology. 2010;**5**:487-496. DOI: 10.1038/nnano.2010.89

[26] Wilson NR, Macpherson JV. Carbon nanotube tips for atomic force microscopy. Nature Nanotechnology. 2009;**4**:483-491. DOI: 10.1038/nnano.2009.154

[27] Lin YM, Dimitrakopoulos C, Jenkins KA, Farmer DB, Chiu HY, Grill A, et al. 100GHz transistor from wafer-scale epitaxial graphene. Science. 2010;**327**:662. DOI: 10.1126/science.1184289

[28] Yan Z, Peng Z, Tour JM. Chemical vapor deposition of graphene single crystals. Accounts of Chemical Research. 2014;**47**:1327-1337. DOI: 10.1021/ar4003043

[29] Su CY, Lu AY, Xu Y, Chen FR, Khlobystov AN, Li LJ. High-quality thin graphene films from fast electrochemical exfoliation. ACS Nano. 2011;**5**:2332-2339. DOI: 10.1021/nn200025p

[30] Hernandez Y, Nicolosi V, Lotya M, Blighe FM, Sun Z, De S, et al. High-yield production of graphene by liquid-phase exfoliation of graphite. Nature Nanotechnology. 2008;**3**:563-568. DOI: 10.1038/nnano.2008.215

[31] Sutter PW, Flege JI, Sutter EA. Epitaxial graphene on ruthenium. Nature Materials. 2008; **7**:406-411. DOI: 10.1038/nmat2166

[32] Berger C, Song Z, Li X, Wu X, Brown N, Naud C, et al. Electronic confinement and coherence in patterned epitaxial graphene. Science. 2006;**312**:1191-1196. DOI: 10.1126/science.1125925

[33] Emtsev KV, Speck F, Seyller T, Ley L, Riley JD. Interaction, growth, and ordering of epitaxial graphene on SiC{0001} surfaces: A comparative photoelectron spectroscopy study. Physical Review B. 2008;**77**:155303. DOI: 10.1103/PhysRevB.77.155303

[34] Hass J, WAd H, Conrad EH. The growth and morphology of epitaxial multilayer graphene. Journal of Physics. Condensed Matter. 2008;**20**:323202. DOI: 10.1088/0953-8984/20/32/323202

[35] Su CY, Xu Y, Zhang W, Zhao J, Liu A, Tang X, et al. Highly efficient restoration of graphitic structure in graphene oxide using alcohol vapors. ACS Nano. 2010;**4**:5285-5292. DOI: 10.1021/nn10169m

[36] Williams G, Seger B, Kamat PV. TiO_2-graphene nanocomposites UV-assisted photocatalytic reduction of graphene oxide. ACS Nano. 2008;**2**:1487-1491. DOI: 10.1021/nn800251f

[37] Green AA, Hersam MC. Solution phase production of graphene with controlled thickness via density differentiation. Nano Letters. 2009;**9**:4031-4036. DOI: 10.1021/nl902200b

[38] Cote LJ, Kim F, Huang J. Langmuir-Blodgett assembly of graphite oxide singl layers. Journal of the American Chemical Society. 2008;**131**:1043-1049. DOI: 10.1021/ja806262m

[39] Li D, Müller MB, Gilje S, Kaner RB, Wallace GG. Processable aquaous dispersions of graphene nanosheets. Nature Nanotechnology. 2008;**3**:101-105. DOI: 10.1038/nnano.2007.451

[40] Gao W, Alemany LB, Ci L, Ajayan PM. New insights into the structure and reduction of graphite oxide. Nature Chemistry. 2009;**1**:403-408. DOI: 10.1038/nchem.281

[41] Joshi RK, Alwarappan S, Yoshimura M, Sahajwalla V. Graphene oxide: The new membrane material. Applied Materials Today. 2015;**1**:1-12. DOI: 10.1016/j.apmt.2015.06.002

[42] Coraux J, Diaye ATN, Busse C, Michely T. Structural coherency of graphene on Ir(111). Nano Letters. 2008;**8**:565-570. DOI: 10.1021/nl0728874

[43] Lee Y, Bae S, Jang H, Jang S, Zhu SE, Sim SH, et al. Wafer-scale synthesis and transfer of graphene films. Nano Letters. 2010;**10**:490-493. DOI: 10.1021/nl903272n

[44] Reina A, Jia X, Ho J, Nezich D, Son H, Bulovic V, et al. Large area, few-layer graphene films on arbitrary substrates by chemical vapor deposition. Nano Letters. 2008;**9**:30-35. DOI: 10.1021/nl801827v

[45] Li X, Cai W, An J, Kim S, Nah J, Yang D, et al. Large-area synthesis of high-quality and uniform graphene films on copper foils. Science. 2009;**324**:1312-1314. DOI: 10.1126/science.1171245

[46] Lee S, Lee K, Zhong Z. Wafer scale homogeneous bilayer graphene films by chemical vapor deposition. Nano Letters. 2010;**10**:4702-4707. DOI: 10.1021/nl1029978

[47] Yan K, Peng H, Zhou Y, Li H, Liu Z. Formation of bilayer Bernal graphene: Layer-by-layer epitaxy via chemical vapor deposition. Nano Letters. 2011;**11**:1106-1110. DOI: 10.1021/nl104000b

[48] Sun Z, Yan Z, Yao J, Beitler E, Zhu Y, Tour JM. Growth of graphene from solid carbon sources. Nature. 2010;**468**:549-552. DOI: 10.1038/nature09579

[49] Chen Y, Gong XZ, Gai JG. Progress and challenges in transfer of large-area graphene films. Advancement of Science. 2016;**3**:1500343. DOI: 10.1002/advs.201500343

[50] Sun J, Deng S, Guo W, Zhan Z, Deng J, Xu C, et al. Electrochemical bubbling transfer of graphene using a polymer support with encapsulated air gap as permeation stopping layer. Journal of Nanomaterials. 2016;**2016**:1-7. DOI: 10.1155/2016/7024246

[51] Cherian CT, Giustiniano F, Martin-Fernandez I, Andersen H, Balakrishnan J, Özyilmaz B. Bubble-free electrochemical delamination of CVD graphene films. Small. 2015;**11**: 189-194. DOI: 10.1002/smll.201402024

[52] Mafra D, Ming T, Kong J. Facial graphene transfer directly to target substrates with a reusable metal catalyst. Nanoscale. 2015;**7**:14807-14812. DOI: 10.1039/C5NR3892H

[53] Wang Y, Zheng Y, Xu X, Dubuisson E, Bao Q, Lu J, et al. Electrochemical delamination of CVD-grown graphene film: Toward the recyclable use of copper catalyst. ACS Nano. 2011;**5**:9927-9933. DOI: 10.1021/nn203700w

[54] Gao L, Ren W, Xu H, Jin L, Wang Z, Ma T, et al. Repeated growth and bubbling transfer of graphene with millimetre-size single-crystal grains using platinum. Nature Communications. 2012;**3**:699. DOI: 10.1038/ncomms1702

[55] Li X, Cai W, Colombo L, Ruoff RS. Evolution of graphene growth on Ni and Cu by carbon isotope labeling. Nano Letters. 2009;**9**:4268-4272. DOI: 10.1021/nl902515k

[56] Wang H, Wang G, Bao P, Yang S, Zhu W, Xie X, et al. Controllable synthesis of submilimeter single-crystal monolayer graphene domains on copper foils by suppressing nucleation. Journal of the American Chemical Society. 2012;**134**:3627-3630. DOI: 10.1021/ja2105976

[57] Eres G, Regmi M, Rouleau CM, Chen J, Ivanov IN, Puretzky AA, et al. Cooperative island growth of large-area single-crystal graphene on copper using chemical vapor deposition. ACS Nano. 2014;**8**:5657-5669. DOI: 10.1021/nn500209d

[58] Wang C, Chen W, Han C, Wang G, Tang B, Tang C, et al. Growth of millimeter-size single crystal graphene on Cu foils by circumfluence chemical vapor deposition. Scientific Reports. 2014;**4**:4537. DOI: 10.1038/srep04537

[59] Li X, Magnuson CW, Venugopal A, Tromp RM, Hannon JB, Vogel EM, et al. Large-area graphene single crystals grown by low-pressure chemical vapor deposition of methane on copper. Journal of the American Chemical Society. 2011;**133**:2816-2819. DOI: 10.1021/ja109793s

[60] Chen S, Ji H, Chou H, Li Q, Li H, Suk JW, et al. Milimeter-size single-crystal graphene by suppressing evaporative loss of Cu during low pressure chemical vapor deposition. Advanced Materials. 2013;**25**:2062-2065. DOI: 10.1002/adma.201204000

[61] Mohsin A, Liu L, Liu P, Deng W, Ivanov IN, Li G, et al. Synthesis of miloimeter-size hexagon-shaped graphene single crystals on resolidified copper. ACS Nano. 2013;**7**:8924-8931. DOI: 10.1021/nn4034019

[62] Wu T, Ding G, Shen H, Wang H, Sun L, Jiang D, et al. Triggering the continuous growth of growth toward milimeter-sized grains. Advanced Functional Materials. 2013;**23**: 198-203. DOI: 10.1002/adfm.201201577

[63] Gan L, Luo Z. Turning off hydrogen to realize seeded growth of subcentimeter single-crystal graphene grains on copper. ACS Nano. 2013;**7**:9480-9488. DOI: 10.1021/nn404 393b

[64] Zhou H, Yu WJ, Liu L, Cheng R, Chen Y, Huang X, et al. Chemical vapour deposition growth of large single crystals of monolayer and bilayer graphene. Nature Communications. 2013;**4**:2096. DOI: 10.1038/ncomms3096

[65] Hao Y, Bharathi MS, Wang L, Liu Y, Chen H, Nie S, et al. The role of surface oxygen in the growth of large single-crystal gtaphene on copper. Science. 2013;**342**:720-723. DOI: 10.1126/science.1243879

[66] Nguyen VL, Shin BG, Duong DL, Kim ST, Perello D, Lim YJ, et al. Seamless stiching of graphene domains on polished copper (111) foil. Advanced Materials. 2015;**27**:1376-1382. DOI: 10.1002/adma.201404541

[67] Kim K, Lee Z, Regan W, Kisielowski C, Crommie MF, Zettl A. Grain bourdary mapping in polycrystalline graphene. ACS Nano. 2011;**5**:2142-2146

[68] Huang PY, Vargas CSR, van der Zande AM, Whitney WS, Levendorf MP, Kevek JW, et al. Grains and grain boundaries in single-layer graphene atomic patchwork quilts. Nature. 2011;**469**:389-392

[69] Rasool HI, Ophus C, Klug WS, Zettl A, Gimzewski JK. Measurement of the intrinsic strength of crystalline and polycrystalline graphene. Nature Communications. 2013;**4**: 2811. DOI: 10.1038/ncomms3811

[70] Lee C, Wei X, Kysar JW, Hone J. Measurement of the elastic properties and intrinsic strength of monolayer graphene. Science. 2008;**321**:385-388. DOI: 10.1126/science.1157996

[71] Tuan DV, Kotakoski J, Louvet T, Ortmann F, Meyer JC, Roche S. Scaling properties of charge transport in polycrystalline graphene. Nano Letters. 2013;**13**:1730-1735. DOI: 10.1021/nl400321r

[72] Zhang H, Lee G, Gong C, Colombo L, Cho K. Grain boundary effect on electrical transport properties of graphene. Journal of Physical Chemistry C. 2014;**118**:2338-2343. DOI: 10.1021/jp411464w

[73] Boukhvalov DW, Katsnelson MI. Chemical functionalization of graphene with defects. Nano Letters. 2008;**8**:4373-4379. DOI: 10.1021/nl802234n

[74] Cummings AW, Duong DL, Nguyen VL, Tuan DV, Kotakoski J, Vargas JEB, et al. Charge transport in polycrystalline graphene: Challenges and opportunities. Advanced Materials. 2014;**26**:5079-5094. DOI: 10.1002/adma.201401389

[75] Chen JH, Li L, Cullen WG, Williams ED, Fuhrer MS. Tunable Kondo effect in graphene with defects. Nature Physics. 2011;**7**:535-538. DOI: 10.1038/nphys1962

[76] Gogotsi Y. Nanomaterials Handbook. Boca Raton, Florida, United States: CRC Press; 2006

[77] Blocher JM, Browning MF, Barrett DM. Emergent Process Methods for High-Technology. Berlin, Germany: Ceramics. Springer; 1984. pp. 299-316

[78] Morosanu CE. Thin Films by Chemical Vapour Deposition. Elsevier; 1990. pp. 1-717

[79] Bhaviripudi S, Jia X, Dresselhaus MS, Kong J. Role of kinetic factors in chemical vapor deposition synthesis of uniform large area graphene using copper catalyst. Nano Letters. 2010;**10**:4128-4133. DOI: 10.1021/nl102355e

[80] Miao C, Zheng C, Liang O, Xie YH. Physics and Applications of Graphene-Experiments, Book Chapter. Chemical Vapor Deposition of Graphene. US: InTech; 2011

[81] Bae S, Kim H, Lee Y, Xu X, Park JS, Zheng Y, et al. Roll-to-roll production of 30-inch graphene films for transparent electrodes. Nature Nanotechnology 2010;**5**:574-578. DOI: 10.1038/nnano.2010.132

[82] Yu Q, Lian J, Siriponglert S, Li H, Chen YP, Pei SS. Graphene segregated on Ni surfaces and transferred to insulators. Applied Physics Letters. 2008;**93**:113103. DOI: 10.1063/1.2982585

[83] Kobayashi T, Bando M, Kimura N, Shimizu K, Kadono K, Umezu N, et al. Production of a 100-m-long high-quality graphene transparent film by roll-to-roll chemical vapor deposition and transfer process. Applied Physics Letters. 2013;**102**:023112. DOI: 10.1063/1.4776707

[84] Boyd DA, Lin WH, Hsu CC, Teague ML, Chen CC, Lo YY, et al. Single step deposition of high-mobility graphene at reduced temperatures. Nature Communications. 2015;**6**:6620. DOI: 10.1038/ncomms7620

[85] Jang J, Son M, Chung S, Kim K, Cho C, Hun LB, et al. Low-temperature-grown continuous graphene films from benzene by chemical vapor deposition at ambient pressure. Scientific Reports. 2015;**5**:17955. DOI: 10.1038/srep17955

[86] Gong Y, Zhang X, Liu G, Wu L, Geng X, Long M, et al. Layer-controlled and wafer-scale synthesis of uniform and high-quality graphene films on a polycrystalline nickel catalyst. Advanced Functional Materials. 2012;**22**:3153-3159. DOI: 10.1002/adfm.201200388

[87] Tu Z, Liu Z, Li Y, Yang F, Zhang L, Zhao Z, et al. Controllable growth of 1-7 layers of graphene by chemical vapour deposition. Carbon. 2014;**73**:252-258. DOI: 10.1016/j.carbon.2014.02.061

[88] Suk JW, Kitt A, Magnuson CW, Hao Y, Ahmed S, An J, et al. Transfer of CVD-grown monolayer graphene onto arbitrary substrates. ACS Nano. 2011;**5**:6916-6924. DOI: 10.1021/nn201207c

[89] Yan Z, Lin J, Peng Z, Sun Z, Zhu Y, Li L, et al. Toward the synthesis of wafer-scale single-crystal graphene on copper foils. ACS Nano. 2012;**6**:9110-9117. DOI: 10.1021/nn303352k

[90] Barcenas AM, Robles JFP, Vorobiev YV, Soto NO, Mexicano A, Garcia AG. Graphene synthesis using a CVD reactor and a discontinuous feed of gas precursor at atmospheric pressure. Journal of Nanomaterials. 2018;**2018**:1-11. DOI: 10.1155/2018/3457263

[91] Wang S, Hibino H, Suzuki S, Yamamoto H. Atmospheric pressure chemical vapor deposition growth of millimeter-scale single graphene on the copper surface with a native oxide layer. Chemistry of Materials. 2016;**28**:4893-4900. DOI: 10.1021/acs.chemmater.6b00252

[92] Campos-Delgado J, Botello-Mendez AR, Algara-Siller G, Hackens B, Pardoen T, Kaiser U, et al. CVD synthesis of mono and few-layer graphene using alcohols at low hydrogen concentration and atmospheric pressure. Chemical Physics Letters. 2013;**584**:142-146. DOI: 10.1016/j.cplett.2013.08.031

[93] Xu X, Zhang Z, Qiu L, Zhuang J, Zhang L, Wang H, et al. Ultrafast growth of single-crystal graphene assisted by a continuous oxygen supply. Nature Nanotechnology. 2016;**11**:930-935. DOI: 10.1038/nnano.2016.132

[94] Wu X, Zhong G, D'Arsie L, Sugime H, Esconjauregui S, Robertson AW, et al. Growth of continuous monolayer graphene with millimeter-sized domains using industrially safe conditions. Scientific Reports. 2016;**6**:21152. DOI: 10.1038/srep21152

[95] Mohsin A, Liu L, Liu P, Deng W, Ivanov IN, Li G, et al. Synthesis of millimeter-size hexagon-shaped graphene single crystals on resolidified copper. ACS Nano. 2013;**7**:8924-8931. DOI: 10.1021/nn4034019

[96] Hess DW, Jensen KF, Anderson TJ. Chemical Vapor Deposition. 2011. DOI: 10.1515/revce.1985.3.2.97

[97] Ishizaka A, Shiraki Y. Low-temperature surface cleaning of silicon and itsapplication to silicon MBE. Journal of the Electrochemical Society. 1986;**133**:666-671. DOI: 10.1149/1.2108651

[98] Kidambi PR, Ducati C, Dlubak B, Gardiner D, Weatherup RS, Martin MB, et al. The parameter space of graphene chemical vapor deposition on polycrystalline Cu. Journal of Physical Chemistry C. 2012;**116**:22492-22501. DOI: 10.1021/jp303597m

[99] Sun H, Han Y, Wu J, Lu Y, Xu J, Luo Y, et al. Cooling growth of milimeter-size single0-crystal bilayer graphene at atmospheric pressure. Journal of Physical Chemistry C. 2016; **120**:13596-13603. DOI: 10.1021/acs.jpcc.6b04105

[100] Qaisi RM, Smith CE, Hussain MM. Atmospheric pressure chemical vapor deposition (APCVD) grown bi-layer graphene transistor characteristics at high temperature. Physica Status Solidi RRL: Rapid Research Letters. 2014;**8**:621-624. DOI: 10.1002/pssr.201409100

IntechOpen